Acclimation to Very Low CO_2: Contribution of Limiting CO_2 Inducible Proteins, LCIB and LCIA, to Inorganic Carbon Uptake in *Chlamydomonas reinhardtii*[1][OPEN]

Yingjun Wang* and Martin H. Spalding*

Department of Genetics, Development and Cell Biology, Iowa State University, Ames, Iowa 50011

ORCID ID: 0000-0002-6332-9706 (Y.W.).

The limiting-CO_2 inducible CO_2-concentrating mechanism (CCM) of microalgae represents an effective strategy to capture CO_2 when its availability is limited. At least two limiting-CO_2 acclimation states, termed low CO_2 and very low CO_2, have been demonstrated in the model microalga *Chlamydomonas reinhardtii*, and many questions still remain unanswered regarding both the regulation of these acclimation states and the molecular mechanism underlying operation of the CCM in these two states. This study examines the role of two proteins, Limiting CO_2 Inducible A (LCIA; also named NAR1.2) and LCIB, in the CCM of *C. reinhardtii*. The identification of an *LCIA-LCIB* double mutant based on its inability to survive in very low CO_2 suggests that both LCIA and LCIB are critical for survival in very low CO_2. The contrasting effects of individual mutations in *LCIB* and *LCIA* compared with the effects of *LCIB-LCIA* double mutations on growth and inorganic carbon-dependent photosynthetic O_2 evolution reveal distinct roles of LCIA and LCIB in the CCM. Although both LCIA and LCIB are essential for very low CO_2 acclimation, LCIB appears to function in a CO_2 uptake system, whereas LCIA appears to be associated with a HCO_3^- transport system. The contrasting and complementary roles of LCIA and LCIB in acclimation to low CO_2 and very low CO_2 suggest a possible mechanism of differential regulation of the CCM based on the inhibition of HCO_3^- transporters by moderate to high levels of CO_2.

The CO_2 concentration in Earth's atmosphere has declined significantly since the origin of photosynthesis, and the current atmospheric CO_2 level is a major limiting factor for optimal photosynthesis in many plant species. Rubisco, the central enzyme catalyzing CO_2 assimilation, has a low affinity for CO_2 and a slow catalytic turnover rate for the carboxylation reaction, possibly as an evolutionary relic, and also catalyzes the competing oxygenation reaction between O_2 and ribulose-1,5-bisphosphate that releases fixed CO_2 through photorespiration. As a result, several adaptive strategies have evolved to improve photosynthetic efficiency by raising the CO_2 concentration at the site of Rubisco to increase the carboxylation rates and to suppress the wasteful photorespiration pathway. Among them, the cyanobacterial/microalgal CO_2-concentrating mechanism (CCM) appears to be one of the most effective strategies for CO_2 enrichment. These CCMs deploy diverse, active inorganic carbon (Ci) uptake systems, allowing cells to accumulate intracellular Ci up to 1,000-fold from low CO_2 environments (Badger and Price, 2003; Moroney and Ynalvez, 2007; Price et al., 2008; Spalding, 2008). Because microalgae and cyanobacteria contribute a great portion of global CO_2 sequestration through photosynthesis (Behrenfeld et al., 2001), and have shown enormous potential as an alternative future energy source (Sheehan et al., 1998; Wijffels and Barbosa, 2010), enhanced knowledge of the microalgal CCM will provide not only insights into the CCM's influences on natural environments, but also guidance for the potential application of bioengineering approaches to enhance biomass productivity in economically important algae strains, or to improve photosynthetic carbon fixation in crop species that lack a CCM.

Although microalgal and cyanobacterial CCMs exhibit a very high level of diversity with regard to components and mechanisms (Badger and Spalding, 2000), these CCMs share some major molecular characteristics, including Rubisco sequestration in a specialized microcompartment, catalyzed interconversion of Ci species by carbonic anhydrase (CA), and energy-dependent, active Ci uptake systems. The eukaryotic CCM has been extensively studied in the model organism *Chlamydomonas reinhardtii* during the last 3 to 4 decades. Compared with the prokaryotic, cyanobacterial CCM, the eukaryotic, microalgal CCM appears complex because of the involvement of additional subcellular compartments and regulatory systems (Wang et al., 2011). Some areas of uncertainty regarding key features of the microalgal CCM remain to be addressed. First, Ci, including the charged species, bicarbonate (HCO_3^-), must cross both the plasma membrane and the chloroplast envelope to

[1] This work was supported by the U.S. Department of Energy, Office of Science (grant no. DEFG02–12ER16335 to Y.W. and M.H.S.) and the National Science Foundation, Directorate for Biological Sciences (grant no. MCB–0952323 to M.H.S.).

* Address correspondence to wangyj@iastate.edu and mspaldin@iastate.edu.

The author responsible for distribution of materials integral to the findings presented in this article in accordance with the policy described in the Instructions for Authors (www.plantphysiol.org) is: Yingjun Wang (wangyj@iastate.edu).

Y.W. and M.H.S. designed the experiments, analyzed the data, and wrote the article; Y.W. performed most of the experiments.

[OPEN] Articles can be viewed online without a subscription.

www.plantphysiol.org/cgi/doi/10.1104/pp.114.248294

reach Rubisco, yet the roles, if any, of proposed and confirmed Ci transporters, including the plasma membrane proteins HLA3 and Limiting CO_2 Inducible1 (LCI1) and the chloroplast envelope proteins LCIA (NAR1.2), CCP1, and CCP2 (Im and Grossman, 2002; Miura et al., 2004; Pollock et al., 2004; Mariscal et al., 2006; Duanmu et al., 2009a; Ohnishi et al., 2010), in acclimation and Ci uptake under different limiting CO_2 conditions are not yet clearly defined. Second, previous physiological studies have demonstrated that active uptake of both CO_2 and HCO_3^- occurs in *C. reinhardtii* (Moroney and Tolbert, 1985; Sültemeyer et al., 1989), but the molecular components and the underlying mechanism responsible for active CO_2 uptake are still largely unknown. Third, the tight regulation of CCM functional components is still not well understood (Spalding et al., 2002). Physiological studies in wild-type *C. reinhardtii* cells have suggested that within the range of so-called limiting or low CO_2 (the meaning of low CO_2 is not universally defined in many previous publications, often ranging from air level of CO_2 to nearly zero CO_2), at least two distinct acclimation states, low CO_2 (approximately 0.03%–0.5%) and very low CO_2 (<0.02%), can be defined (Vance and Spalding, 2005). However, recent transcriptome studies (Brueggeman et al., 2012; Fang et al., 2012) failed to identify any changes that occur at the transcription abundance level between low CO_2 and very low CO_2 conditions, so it is still unclear how the CCM is differentially regulated between these two limiting CO_2 acclimation states.

The first line of clear genetic evidence showing multiple, limiting-CO_2 acclimation states came from identification of mutants with an *air dier* growth phenotype (Wang and Spalding, 2006); these mutants die in air level of CO_2 (0.03%–0.05%) but can survive in either high CO_2 (5%) or very low CO_2 (<0.02%), and their ability to accumulate Ci is severely compromised in low CO_2 but fairly normal in very low CO_2. The mutation causing this *air dier* phenotype has been unequivocally linked to the *LCIB* gene (Wang and Spalding, 2006), which encodes a novel chloroplast protein that forms a heteromultimeric complex with its close homolog LCIC (Yamano et al., 2010; Wang and Spalding, 2014). It is unclear how LCIB is involved in Ci accumulation, largely because of its unknown biochemical characteristics and the lack of homologs of known function in other organisms. Genetic analysis of *LCIB/CAH3* double mutants indicated that LCIB functions downstream of CAH3, a thylakoid lumen CA (Duanmu et al., 2009b). Because CAH3 catalyzes dehydration of accumulated HCO_3^- to provide CO_2 for Rubisco inside the pyrenoid (Spalding et al., 1983b; Moroney et al., 2011), it has been hypothesized that LCIB captures CO_2 leaked from the pyrenoid, possibly by unidirectionally hydrating CO_2 back to HCO_3^- (Duanmu et al., 2009b). If this hypothesis is correct, it also implies that LCIB may also function in active Ci accumulation by unidirectionally hydrating externally diffused CO_2 into the stromal HCO_3^- pool (Wang and Spalding, 2014). LCIB and the LCIB/LCIC complex change location within the chloroplast when cells are transferred from low CO_2 (or high CO_2) to very low CO_2 conditions (Yamano et al., 2010; Wang and Spalding, 2014; Yamano et al., 2014), suggesting that a regulatory mechanism exists to regulate the functions of LCIB, possibly associated with low CO_2 and very low CO_2 acclimation states.

The growth phenotype and physiological characteristics of *LCIB* mutants clearly demonstrate that LCIB is indispensable for Ci acquisition in low CO_2, but is dispensable in very low CO_2 when other Ci uptake systems are still functional. It is also clear, however, that even though it is dispensable, LCIB contributes to viability in very low CO_2 (Duanmu et al., 2009a), although neither its level of contribution to nor its precise role in Ci uptake under these conditions has been established. Two putative Ci transporters have been demonstrated to contribute LCIB-independent Ci uptake in *C. reinhardtii*. Knockdown of *HLA3*, a gene encoding an ATP-binding cassette transporter protein, causes growth defects in *LCIB* mutants in very low CO_2 and decreased Ci accumulation especially at a high pH (Duanmu et al., 2009a). HLA3 is predicted to be localized on the plasma membrane, and therefore is very likely involved in HCO_3^- transport at this location. LCIA, another putative Ci transporter that might be involved in Ci uptake in very low CO_2, belongs to a formate-nitrite transporter (FNT) family (Mariscal et al., 2006), and is predicted to be targeted to the chloroplast envelope (Miura et al., 2004). Although it shows significant identity to the *C. reinhardtii* nitrate assimilation-related (NAR) gene family and has also been named *NAR1.2*, unlike other *NAR* genes, *LCIA* expression is regulated by CO_2 but not by nitrogen source (Miura et al., 2004; Mariscal et al., 2006), and introduction of an LCIA gene into *Xenopus laevis* oocytes reportedly increased HCO_3^- uptake (Mariscal et al., 2006). Although no LCIA single knockout or knockdown mutants have been reported, simultaneous co-knockdown of LCIA with HLA3 resulted in decreased Ci accumulation and decreased growth in very low CO_2, especially when combined with *LCIB* mutations (Duanmu et al., 2009a). Although it appears that their contribution to Ci uptake may be important for the growth of *C. reinhardtii* under very low CO_2, HLA3- or LCIA-associated Ci uptake in the absence of LCIB cannot support growth of LCIB mutants in air-level CO_2, as evidenced by the *air dier* phenotype. This suggests that the primary role for these putative Ci transporters may be in very low CO_2 conditions, but it is not clear whether, or how, HLA3 and LCIA are differentially regulated between very low CO_2 and low CO_2.

This study was undertaken primarily to dissect the molecular mechanisms underlying the functional acclimation to very low CO_2 in *C. reinhardtii*. We identified an *LCIA-LCIB* double mutant that is unable to survive in very low CO_2. The effects of the single *LCIB* mutation, the *LCIA* mutation, and the combined *LCIA* and *LCIB* mutations on growth and Ci-dependent photosynthetic O_2 evolution reveal possible functions of LCIB and LCIA in the CCM, and demonstrate that both LCIA and LCIB contribute to Ci acquisition and acclimation under

very low CO_2 conditions but that they play distinct and complementary roles. Analyses of these data also revealed a possible mechanism to explain the curious *air dier* phenotype of *LCIB* mutants and the regulation between low CO_2 and very low CO_2 acclimation states.

RESULTS

Impact of *LCIB* Mutation on Ci-Dependent O_2 Evolution

LCIB mutations cause severe inhibition of Ci uptake and photosynthesis in low CO_2, but appear to have much less impact on photosynthesis in very low CO_2 (Spalding et al., 1983a; Wang and Spalding, 2006; Duanmu et al., 2009a; Yamano et al., 2010; Duanmu and Spalding, 2011). To better understand this dichotomy, we more closely examined the impact of the *LCIB* mutation on very low CO_2 acclimation and Ci species dependence of photosynthesis in the *LCIB* mutant by comparing photosynthetic O_2 evolution in very low CO_2 acclimated cells of the wild type and the *LCIB* mutant *air dier1* (*ad1*; Wang and Spalding, 2006) at two pHs. As shown in Figure 1A, at an acidic pH (pH 6.0), where the relative abundance of CO_2 is higher, O_2 evolution in *ad1* was severely inhibited in 10 to 100 μM Ci but regained wild type rates at 200 μM Ci. However, at pH 7.3, where HCO_3^- is much more abundant than CO_2, O_2 evolution rates in *ad1* were very similar to those of wild-type cells at 0 to 50 μM Ci but were inhibited relative to the wild type in 50 to 200 μM Ci. Furthermore, photosynthetic rates in *ad1* actually decreased as Ci concentration was increased between 50 μM and 200 μM. The different responses of *ad1* at these two pHs suggest that the function of LCIB, which is absent in *ad1*, is Ci species dependent. When the photosynthetic O_2 evolution rates are plotted as a function of the calculated CO_2 or HCO_3^- concentrations (Fig. 1, B and C), the apparent inhibition of O_2 evolution in *ad1* relative to the wild type occurs in the same CO_2 concentration range, but in different total Ci or HCO_3^- concentration ranges, at both pHs, and this CO_2 range corresponds to CO_2 concentrations associated with the low CO_2 acclimation state (Vance and Spalding, 2005), even though the algae were acclimated to very low CO_2. These results suggest that the *LCIB* mutant is compromised strictly in CO_2 uptake and specifically in the low CO_2 range. Furthermore, the different responses of *ad1* at two pHs also suggest that another element, possibly a HCO_3^- transport pathway, is responsible for the apparently normal photosynthetic O_2 evolution at lower Ci concentrations ($<$50 μM at pH 7.3; $<$10 μM at pH 6.0), equivalent to $<$ 7 μM CO_2 at either pH, which corresponds to the range of CO_2 concentrations associated with the very low CO_2 acclimation state (Vance and Spalding, 2005). The rates of photosynthetic O_2 evolution in *ad1* are very similar at either pH when plotted as a function of the HCO_3^- concentration, but not the total Ci or CO_2 concentration (Fig. 1, D–F), which supports the suggestion that a HCO_3^- transport system is responsible for the growth and Ci uptake of the *LCIB* mutant in very low CO_2.

Generation of Additional Mutations in an *LCIB* Mutant Background

Although the LCIB-associated Ci uptake is missing in *LCIB* mutants, other Ci uptake systems appear still functional, as evidenced by the nearly normal photosynthetic rates of *ad1* in the lowest Ci concentrations ($<$50 μM at pH 7.3; $<$10 μM at pH 6.0; Fig. 1A) and by its apparently normal growth in very low CO_2 (Fig. 2). To facilitate identification of Ci uptake systems responsible in *LCIB* mutants for active Ci uptake and growth in very low CO_2, *ad1* was mutagenized by random insertion of an *aminoglycoside 3-phosphotransferase* (*Aph8*) gene-bearing plasmid (Sizova et al., 2001), selected for paromomycin resistance ($para^R$) and screened for inability to grow in very low CO_2. Five mutants with the target phenotype were identified from about 2,000 screened $para^R$ transformants. Whereas *ad1* shows a typical *air dier* growth phenotype and thus can still grow in very low CO_2, these new mutants were unable to grow in either very low CO_2 or low CO_2, but grew as well as the wild type in high CO_2 (Fig. 2). The genomic DNA flanking the *Aph8* insert from these new double mutants was isolated and sequenced, which confirmed that all were independent mutants. One mutant in which the insert was found to have disrupted the *LCIA* gene was named *lab1* (*LCIA-LCIB* double mutant), and was further characterized.

LCIA Mutation in *lab1* Responsible for the Lethal Growth Phenotype in Very Low CO_2

The plasmid bearing *Aph8* in *lab1* is inserted in the sixth exon of *LCIA*, causing a 243 base deletion, including 133 nucleotides in the coding sequence and 110 nucleotides in the 3′ untranslated region (UTR; Fig. 3A). The insertion in *LCIA* was confirmed by PCR with a pair of primers that amplify the genomic DNA in this region (Fig. 3B). In wild-type cells, expression of the LCIA protein is induced by limiting CO_2. However, even though the insertion in *lab1* is located near the 3′ end of *LCIA* and causes a deletion of only 44 C-terminal amino acids, western immunoblots were unable to detect any LCIA protein in *lab1* (Fig. 3C), either because *LCIA* is not properly transcribed or not properly translated or because its transcripts or polypeptides are quickly degraded.

A genetic cross between *lab1* and wild-type strain CC620 was performed to confirm whether the lethal growth phenotype in *lab1* is caused by the mutation in *LCIA*. Because *lab1* has both a *bacterial phleomycin resistance* (*Ble*) gene, (confers zeocin resistance [zeo^R]) insert (causing the *LCIB* deletion) and an *Aph8* insert (causing the *LCIA* truncation), progeny carrying both *LCIB* and *LCIA* mutations were selected for both zeo^R and $para^R$. More than 50 random progeny were tested for growth in different CO_2 concentrations, and all progeny carrying both mutations (confirmed by PCR) showed the same growth phenotype as *lab1* (lethal in both low CO_2 and very low CO_2), indicating that the inability of *lab1* to grow in very low CO_2 is genetically linked to the insertion in *LCIA*. We further cloned a genomic DNA fragment containing the

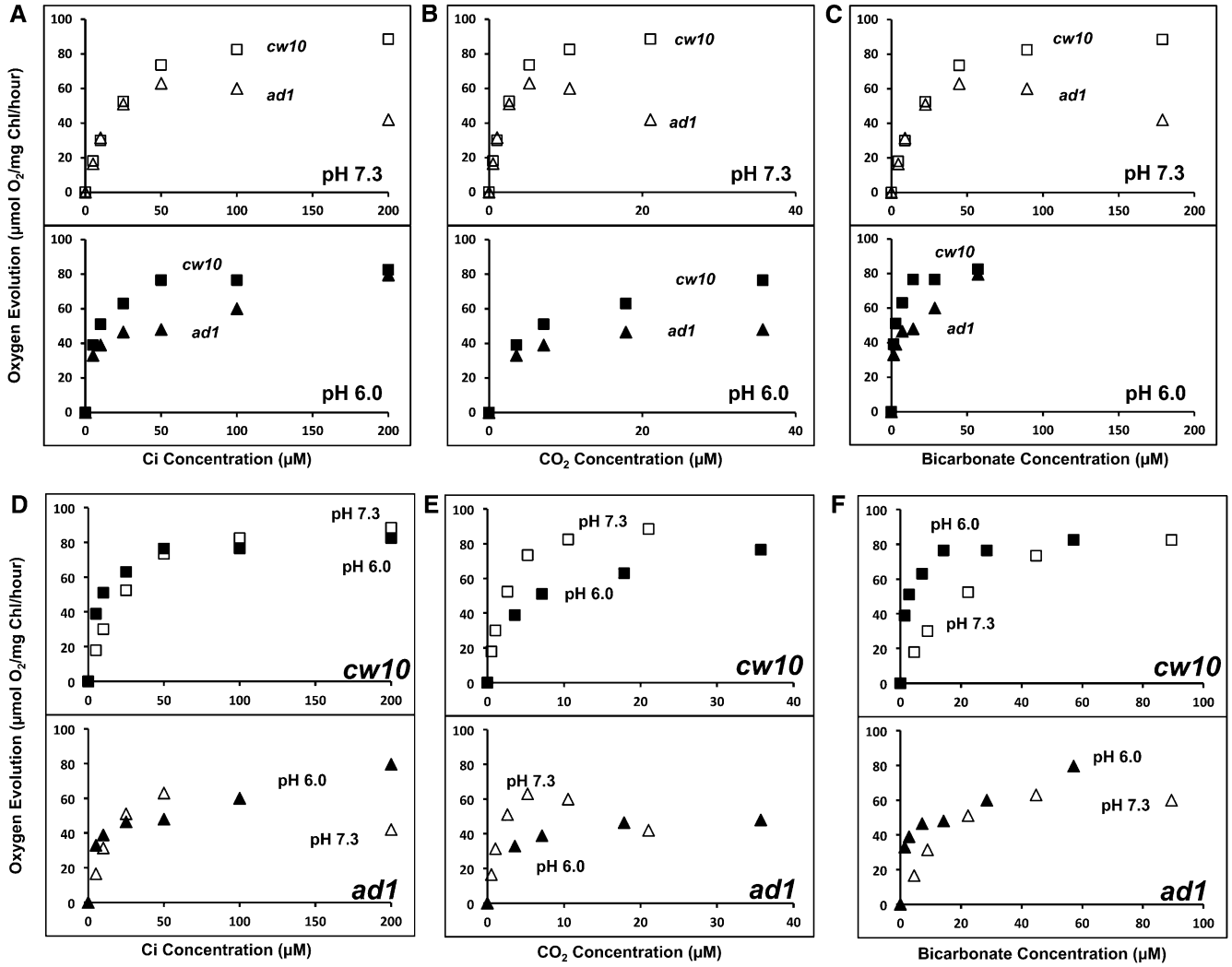

Figure 1. Photosynthetic activity in the wild type and the *LCIB* mutant *ad1*. A, Ci-dependent O_2 evolution at pH 7.3 and 6.0. Strains *cw10* (squares) and *ad1* (triangles) were grown in high CO_2 and then switched to very low CO_2 for 24 h before the measurement. Two hundred units per milliliter of bovine CA was present to ensure the equilibrium of CO_2 and HCO_3^-. B and C, The photosynthetic activities were plotted against CO_2 (B) and HCO_3^- (C) concentrations calculated from total Ci at pH 6.0 (black squares for *cw10* or black triangles for *ad1*) and pH 7.3 (white squares for *cw10* or white triangles for *ad1*). D to F, Comparison of the photosynthetic activities of *cw10* and *ad1* at pH 7.3 and 6.0 plotted against total Ci (D) or CO_2 (E) and HCO_3^- (F) concentrations calculated from total Ci. The experiments showed similar results with two independent cultures, although results from only one experiment are shown. Each data point represents an average of three technical replicates, and the coefficient of variation for each data point, the ratio of the SD ($n = 3$) to the average, is less than 10% for all data. The O_2 evolution rates in *cw10* and *ad1* at 4,000 μM Ci are as follows: in pH 7.3, *cw10* (101 ± 2) and *ad1* (97 ± 5); and in pH 6.0, *cw10* (93 ± 3) and *ad1* (91 ± 6).

wild-type *LCIA* gene, including 1.1 kb of the upstream sequence (presumably including the *LCIA* promoter region) and the entire 3′ UTR, introduced this gene into the *lab1* mutant, and found that this *LCIA* genomic clone complemented growth of *lab1* in very low CO_2. All complemented lines restored the *air dier* growth phenotype of the host strain *ad1* (Fig. 2), and the presence of a wild-type *LCIA* gene and the expression of LCIA protein induced by limiting CO_2 in these lines were confirmed by PCR and western immunoblots (Fig. 3D). These results demonstrate that the lethal growth phenotype in very low CO_2 in the *LCIA-LCIB* double mutant is caused by the *LCIA* mutation.

Defective Photosynthesis in *lab1* Double Mutants

The inability of *lab1* to grow in very low CO_2 suggests that photosynthesis driven by active Ci uptake systems may be defective. Compared with that of the wild type, Ci-dependent O_2 evolution in *lab1* was severely inhibited in Ci concentrations ≤ 200 μM at pH 7.3 and markedly decreased in Ci concentrations ≤ 100 μM

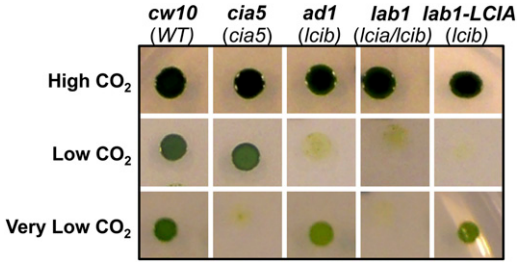

Figure 2. Identification of *lab1*, an *LCIA-LCIB* double mutant. A, Growth of the wild type (*cw10*) and mutant strains on minimal medium agar plates in different concentrations of CO_2: high CO_2 (5%), low CO_2 (0.04%), and very low CO_2 (0.01%). The mutant genes are shown in parentheses below the strain names. *lab1-LCIA* is a cell line generated from *LCIA*-complemented *lab1*. Strain *cia5* is a classic mutant lacking a limiting CO_2 acclimation response. WT, Wild type.

at pH 6.0 (Fig. 4A). Photosynthetic O_2 evolution in *lab1* was similar at either pH when plotted as a function of the calculated CO_2 concentration (Fig. 4B), suggesting that photosynthetic CO_2 assimilation remaining in the absence of both LCIB and LCIA is largely supported through Ci diffusion (Spalding and Ogren, 1983). Because photosynthesis in *LCIB* single mutants appears to be dependent on HCO_3^- uptake, as evidenced by the apparent dependence of photosynthetic O_2 evolution in *ad1* on the concentration of HCO_3^- (Fig. 1C), the highly reduced and apparently CO_2-dependent photosynthesis in *LCIA-LCIB* double mutants implies that LCIA is required for much of the active HCO_3^- uptake in *ad1*.

Decreased HCO_3^--Dependent Photosynthesis in *LCIA* Single Mutants

The impacts of an *LCIA* single mutation on growth and photosynthesis were evaluated in progeny bearing only the *LCIA* mutation. These were identified as para^R but zeocin-sensitive progeny from the genetic cross of *lab1* with CC620 described above. PCR and western-blot analysis confirmed that these para^R but zeocin-sensitive progeny carry the *LCIA* mutation but retain the wild-type *LCIB* gene (Fig. 5, B and C). In contrast with *lab1* or *ad1*, the *LCIA* single-gene mutants did not show any obvious growth defect in spot tests at either low CO_2 or very low CO_2 (Fig. 5A), indicating that loss of LCIA alone has no gross impact on growth and photosynthesis under these conditions.

Ci-dependent photosynthetic O_2 evolution in several *LCIA* mutant progeny was similar to that of wild-type cells at pH 7.3, as illustrated by the comparison between one *LCIA* mutant, *lcia*90, and its wild-type parent CC620 (Fig. 6). Although the Ci-dependent photosynthetic activities of *lcia*90 and the wild type are very similar at pH 7.3, photosynthesis was significantly inhibited in *lcia*90 relative to the wild type at pH 9.0. Because almost all Ci at pH 9 is in the form of HCO_3^-, decreased photosynthesis under these conditions is consistent with the mutation in *LCIA* causing a defect in active HCO_3^- uptake.

DISCUSSION

We have demonstrated that two *C. reinhardtii* proteins, LCIA and LCIB, both contribute to CCM-mediated Ci assimilation in very low CO_2, exemplified by growth and photosynthesis of mutants defective in *LCIB* and *LCIA*. Whereas *LCIB* or *LCIA* single-gene mutants show no obvious growth defects in very low CO_2, combination of these mutations in the *LCIA-LCIB* double mutant results in a lethal phenotype under very low CO_2 conditions. This demonstrates that LCIB- and LCIA-associated Ci uptake systems act either complementarily or synergistically in Ci uptake. The effects of *LCIA* or *LCIB* single mutations and *LCIA-LCIB* double mutations on Ci-dependent photosynthesis at different pHs reveal that LCIA and LCIB play distinct roles in different active Ci uptake processes. Whereas LCIB appears involved in active CO_2 uptake, LCIA is more likely involved in a HCO_3^- transport pathway.

LCIB-Based CO_2 Uptake System

The essentiality of LCIB in CCM-mediated Ci accumulation was demonstrated by a number of earlier studies with *LCIB* mutants, and LCIB was previously proposed to function in direct Ci transport, Ci transport regulation, recapture of CO_2 escaping from the pyrenoid

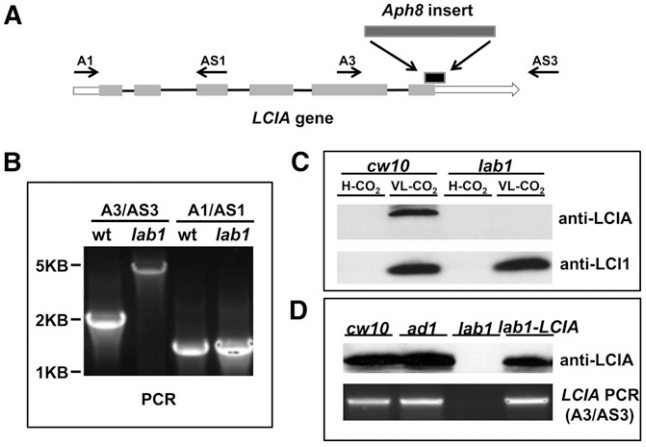

Figure 3. Analysis of *lab1*, an *LCIA-LCIB* double mutant. A, Insertion of *Aph8* in *lab1*. The region of deletion in *LCIA* caused by the Aph8 insertion is shown with a black box above the *LCIA* gene. B, Amplification of genomic DNA fragments in *LCIA* by PCR from *cw10* and *lab1*. The locations of primers in *LCIA* are shown in A. The primers A1 and AS1 were used to amplify a region without insertion; A3 and AS3 were used to amplify a region disrupted by the *Aph8* insert in *lab1*, and the larger size of PCR product in *lab1* confirmed the insertion. C, Western-blot analysis of expression of LCIA and LCI1 in cells acclimated to high CO_2 or very low CO_2. LCI1 is a protein encoded by *LCI1*, a limiting CO_2-induced gene, and was used as the control. No difference in LCI1 induction was observed between the wild type and *lab*1. D, Recovery of induced expression of LCIA in *LCIA*-complemented *lab1*. Wild-type *cw10* and mutants *ad1*, *lab1*, and *LCIA*-complemented *lab1* were grown in high CO_2, and then shifted into very low CO_2 for 12 h. LCIA protein was detected by western immunoblots with a specific LCIA antibody.

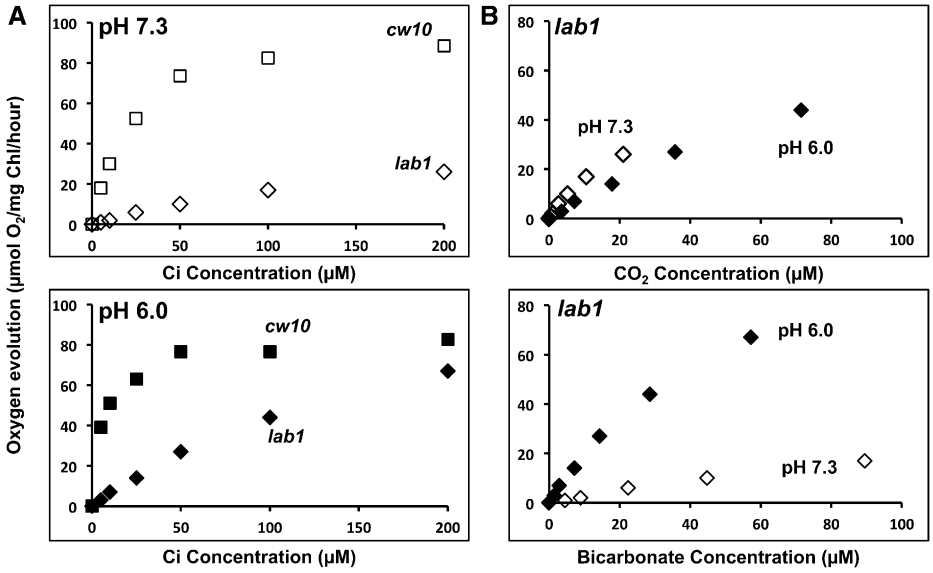

Figure 4. Ci-dependent photosynthetic oxygen evolution in *cw10* and *lab1*. A, Ci-dependent O_2 evolution at pH 7.3 and 6.0. Strains *cw10* (squares) and *lab1* (diamonds) were grown in high CO_2 and then switched to very low CO_2 for 24 h before the measurement. Two hundred units per milliliter of bovine CA was present to ensure the equilibrium of CO_2 and HCO_3^-. B, The photosynthetic activities of *lab1* measured at pH 7.3 (white diamonds) and pH 6.0 (black diamonds) were plotted against CO_2 or HCO_3^- concentration calculated from total Ci. The experiments showed similar results with two independent cultures, although results from only one experiment are shown. Each data point represents an average of three technical replicates, and the coefficient of variation for each data point, the ratio of the SD ($n = 3$) to the average, is less than 10% for all data. The O_2 evolution rates of *lab1* at 4,000 μM Ci are as follows: (78 ± 3) in pH 7.3 and (79 ± 6) in pH 6.0. The rates of *cw10* are the same in Figure 1.

and/or the thylakoid lumen, or physically preventing CO_2 escape from pyrenoids (Spalding et al., 1983a; Miura et al., 2004; Wang and Spalding, 2006, 2014; Duanmu et al., 2009b; Yamano et al., 2010). Here we demonstrate that the absence of LCIB causes photosynthetic defects under low Ci conditions that correlate with CO_2 concentrations. At a slightly acidic pH (pH 6.0), where CO_2 comprises more than one-half of the total Ci, Ci-dependent photosynthetic O_2 evolution in the *LCIB* mutant *ad1* was significantly inhibited at 10 to 100 μM Ci (approximately 7–70 μM CO_2), but at pH 7.3, where HCO_3^- dominates, photosynthetic O_2 evolution was not affected below 50 μM Ci (approximately 6 μM CO_2), but showed progressively greater inhibition at higher Ci concentrations. Yamano et al. (2010) reported an inhibition of photosynthetic O_2 evolution in the *LCIB* mutants above 200 μM Ci at pH 7.8 (approximately 7 μM CO_2), but no obvious inhibition was observed below 100 μM Ci. It is clear that the lack of LCIB in *ad1* results in an apparent inhibition of O_2 evolution at similar CO_2 concentrations regardless of the pH, and that the lower limit of those CO_2 concentrations in all cases (6–7 μM or approximately 0.02%; Fig. 1C) is very similar to the gas-phase CO_2 concentration of 0.02% that we previously defined as the upper limit of the very low CO_2 acclimation state based on physiological characteristics in a wild-type strain and on the *air dier* phenotype (Vance and Spalding, 2005; Wang and Spalding, 2014). Below this CO_2 concentration, *LCIB* mutants grow, and above this concentration, up to at least air CO_2 level (0.03%–0.05% CO_2), *LCIB* mutants cannot survive.

When CO_2 significantly exceeds air CO_2 level, CO_2 diffusion alone may be enough to allow the mutants to survive. The CO_2 concentration at which *LCIB* mutants regained wild-type O_2 evolution rates at pH 6.0 (Fig. 1A; 200 μM Ci, corresponding to 140 μM or 0.42% CO_2,) is also close to the Ci concentration at pH 7.8 where cells were reported by Yamano et al. (2010) to regain wild-type photosynthetic rates (4500 μM Ci at pH 7.8, corresponding to 170 μM or 0.5% CO_2). This CO_2 concentration is also close to the upper limit of the low CO_2 acclimation state according to the previous physiological study with wild-type cells by Vance and Spalding (2005). On the basis of these data, LCIB likely plays a major role in the CCM via active CO_2 uptake, especially in the range of low CO_2 (0.02%–0.5%), although the underlying biochemical mechanism is not clear.

We recently proposed that LCIB may function similarly to the cyanobacterial ChpX/Y proteins in converting CO_2 to HCO_3^- (Duanmu et al., 2009b; Wang and Spalding, 2014). ChpX/Y proteins in cyanobacteria are proposed to convert CO_2 to HCO_3^- unidirectionally, in contrast with the bidirectional activity of CAs, via their linkage to NADH dehydrogenase complexes (Price et al., 2002). If LCIB does function in this manner, it should also accelerate HCO_3^- accumulation by hydrating externally diffused CO_2 in the chloroplast stroma, which has an alkaline pH in light. Although this proposed active role

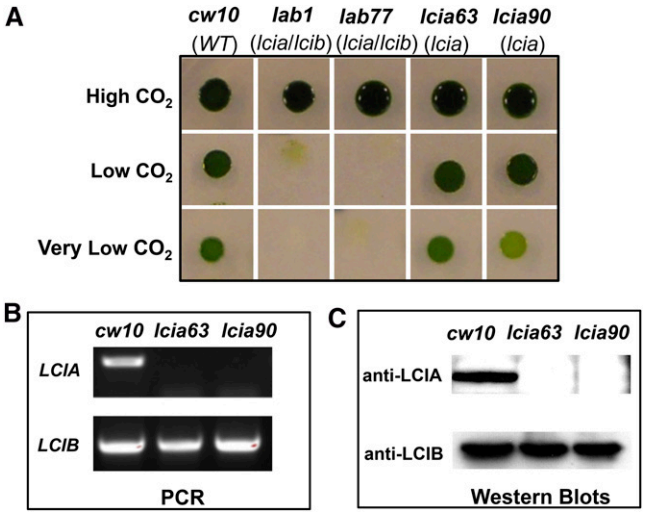

Figure 5. Generation and analysis of LCIA single mutants. A, Growth of the wild type, *lab1* double mutant, and *LCIA* single mutants. Strains *lab77* (an *LCIA-LCIB* double mutant progeny), *lcia63*, and *lcia90* (LCIA single-mutant progeny) were derived from a genetic cross between *lab1* and wild-type strain CC620. B, PCR with specific primers amplifying the disrupted regions in *LCIA* or *LCIB*. C, Western immunoblots with specific LCIA or LCIB antibody. Wild-type cells and mutants *lcia-63* and *lcia90* were grown in high CO_2, and then shifted into very low CO_2 for 12 h prior to analysis. WT, Wild type.

of LCIB in CO_2 uptake into the accumulated HCO_3^- pool is consistent with and can explain the observed physiological characteristics of *LCIB* mutants, *LCIB/CAH3* double mutants (Duanmu et al., 2009b), and *LCIB/LCIA* double mutants, it is still speculative and needs to be rigorously tested at the biochemical level.

Function of LCIA in Ci Uptake

In contrast with the photosynthetic effect of *LCIB* mutations, the impact of an *LCIA* mutation, either alone or in combination with an *LCIB* mutation, on photosynthetic O_2 evolution is more significant at higher pH, indicating that LCIA is likely involved in HCO_3^- uptake. LCIA has a predicted chloroplast envelope location (Miura et al., 2004), which we confirmed by immunolocalization (see Fig. 8A). Although active Ci uptake across the chloroplast envelope has been demonstrated (Sültemeyer et al., 1988; Moroney and Mason, 1991; Amoroso et al., 1998) and LCIA was previously identified as a possible chloroplast envelope Ci transporter (Miura et al., 2004; Mariscal et al., 2006; Duanmu et al., 2009a), no clear, direct evidence links LCIA to active, chloroplast envelope Ci uptake. In addition to the lack of direct evidence for Ci transport by LCIA, other potential Ci transporters, such as CCP1 and CCP2, are also present on the chloroplast envelope (Ramazanov et al., 1993). In addition, chloroplast Ci uptake also might be explained by the activity of LCIB.

LCIA belongs to an FNT family (Mariscal et al., 2006). Multiple recent studies have shown that the bacterial FNT proteins form a pentameric complex with a structure similar to aquaporin and behave more like channels than active transporters (Wang et al., 2009; Lü et al., 2012a, 2013). Nonselective permeability of FNT proteins to several structurally similar small, anionic molecules also has been demonstrated in artificial lipid membranes (Lü et al., 2012b). It seems improbable that LCIA would function as a HCO_3^- channel in the chloroplast envelope, because the membrane potential of the chloroplast envelope is inside negative (Demmig and Gimmler, 1983; Wu et al., 1991; Fuks and Homblé, 1999), meaning that HCO_3^- (or any anion) would have to move against an electrical gradient to enter the chloroplast. However, if LCIA does function as a channel to facilitate passive entry of HCO_3^- into the chloroplast, it would have to depend on the activity of plasma membrane Ci transporters (e.g. HLA3 and LCI1; Duanmu et al., 2009a; Ohnishi et al., 2010) to generate a sufficiently high HCO_3^- concentration in the relatively small volume between the plasma membrane and chloroplast envelope to establish a HCO_3^- concentration gradient sufficient to overcome the electrical gradient and push HCO_3^- across the inner envelope. An LCIA channel would also have to be highly regulated to prevent reversed flow when the HCO_3^- gradient was not favorable for uptake. Ci uptake studies with isolated chloroplasts from *LCIA* mutants and

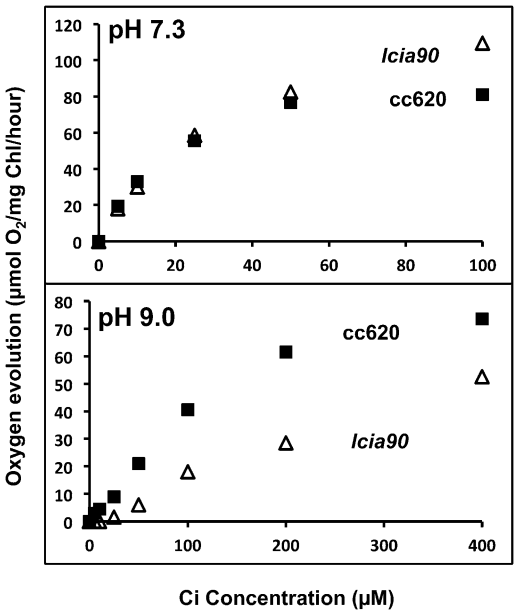

Figure 6. Ci-dependent photosynthesis in the *LCIA* mutant. Ci-dependent photosynthetic O_2 evolution measured at pH 7.3 and 9.0. Strains CC620 (black squares) and *lcia90* (white triangles) were grown in high CO_2 and then switched to very low CO_2 for 24 h before the measurement. The experiments showed similar results with two independent cultures, although results from only one experiment are shown. Each data point represents an average of three technical replicates, and the coefficient of variation for each data point, the ratio of the SD (n = 3) to the average, is less than 10% for all data. The O_2 evolution rates of CC620 and *lcia90* at 4,000 μM Ci are as follows: in pH 7.3, CC620 (95 ± 2) and *lcia90* (132 ± 4); and in pH 9.0, CC620 (87 ± 4) and *lcia90* (112 ± 2).

LCIA overexpression lines will help to clarify whether LCIA is directly responsible for HCO_3^- uptake into chloroplasts and, if so, whether it performs as an active Ci transporter or as an anion channel. Future biochemical, biophysical, and structural characterizations of LCIA will also be required to clarify the molecular mechanism underlying LCIA-associated Ci uptake.

CO_2 Inhibition of LCIA-Mediated Ci Uptake

As shown in Figure 1B, the photosynthetic O_2 evolution in an *LCIB* mutant progressively decreased as the Ci concentration increased beyond 50 μM at pH 7.3. The O_2 evolution rate of *ad1* at 200 μM Ci (approximately 22 μM CO_2) was significantly reduced compared with that at 50 μM at this pH. Yamano et al. (2010) reported similar responses at a higher pH (pH 7.8) in *LCIB* mutants, in which the mutants showed O_2 evolution rates similar to those of the wild type at 0 to 100 μM Ci, but reduced rates at higher Ci concentrations. The most significant inhibition occurred at 500 to 700 μM Ci (approximately 19–27 μM CO_2). In these higher pHs (pH 7.3 or pH 7.8), the dominant Ci species is HCO_3^-, and the reduced activity at higher Ci concentrations cannot be simply explained by a defect in CO_2 uptake caused by an *LCIB* mutation, because the Ci-dependent photosynthetic rates in these mutants should then at least remain constant, if not increase, with increased Ci concentrations. Because it seems clear that an LCIA-associated system contributes significant Ci uptake in cells lacking LCIB, this observed Ci inhibition of photosynthetic O_2 evolution must represent inhibition of LCIA-associated Ci uptake activity.

We reasoned that if LCIA-mediated Ci uptake activity is inhibited by Ci, this should be evident in the calculated difference in photosynthetic activity between *ad1*and *lab1*, which should represent the contribution of LCIA to the photosynthetic performance of *ad1*. When we calculate this LCIA contribution from O_2 evolution data obtained at pH 6.0 and pH 7.3 and plot it as a function of calculated CO_2 and HCO_3^- concentrations (Fig. 7, A and B), it becomes evident that Ci inhibition of LCIA-associated Ci uptake activity responds to CO_2 rather than to either HCO_3^- or total Ci concentrations. Furthermore, the apparent minimum inhibitory CO_2 concentration occurs just above that defined as very low CO_2 (approximately 7 μM CO_2 at room temperature), and becomes more significant at a CO_2 concentration range equivalent to air level (approximately 12 μM CO_2 at room temperature) and above, implying that air level or low CO_2 inhibits the LCIA-associated Ci uptake system.

The Ci response of the *LCIB* mutant at lower pH (pH 6.0) is different from that at higher pH, in that the photosynthetic O_2 evolution rates of *ad1* are inhibited relative to the wild type at pH 6.0 but plateau rather than decreasing with increasing CO_2 concentration, as observed at pH 7.3 (Fig. 1). In this CO_2 concentration range, the rate of O_2 evolution is much higher at pH 7.3 than that at pH 6.0 (Fig. 1B), possibly because the HCO_3^- concentration is higher at pH 7.3 and can support a much higher rate of HCO_3^- transport. Therefore, the inhibition of this higher

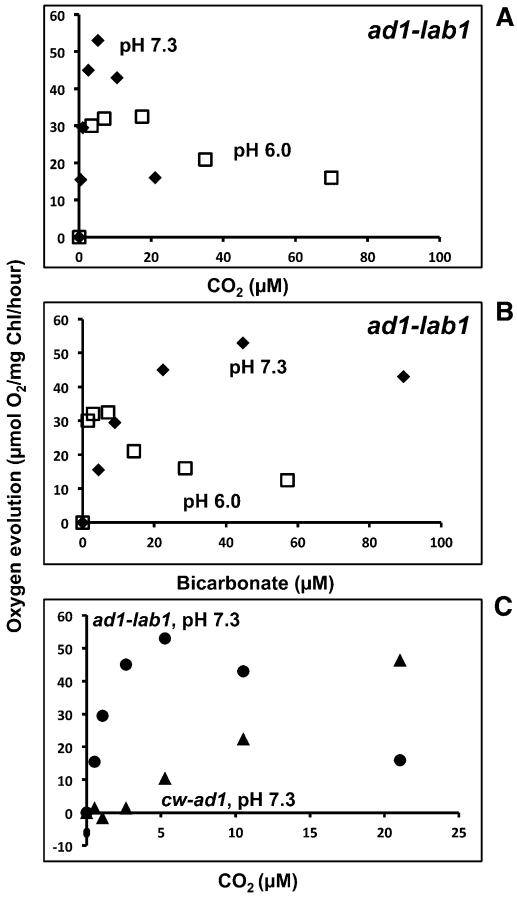

Figure 7. Contributions of LCIA and LCIB to O_2 evolution and CO_2 inhibition of LCIA-dependent photosynthesis. A and B, Contributions to O_2 evolution activities of LCIA and LCIB. Contribution of LCIA to O_2 evolution activities in *ad1* as a function of CO_2 (A) or HCO_3^- (B) concentration at pH 6.0 (white squares) and pH 7.3 (black diamonds). The LCIA contribution was calculated by subtracting photosynthetic O_2 evolution activity in *lab1* from that in *ad1*. C, Contributions of LCIA and LCIB to photosynthesis as a function of the CO_2 concentration. The contribution of LCIA (black circles) was calculated as above, and the contribution of LCIB (black triangles) was calculated by subtracting photosynthetic O_2 evolution activity in *ad1* from that in wild-type (*cw10*) cells. In all cases, CO_2 and HCO_3^- concentrations are calculated from total Ci concentration and pH, assuming that the addition of CA maintains CO_2-HCO_3^- equilibrium.

HCO_3^- transport rate at pH 7.3 has a greater impact on the overall rate of O_2 evolution, resulting in a quantitative decrease in the O_2 evolution rate. The observation that the rate of O_2 evolution at about 20 μM CO_2 is the same at pH 6.0 and pH 7.3 supports this interpretation.

The inhibition of LCIA activity by air level of CO_2 could explain the puzzling *air dier* growth phenotype of *LCIB* mutants, because HCO_3^- uptake associated with LCIA (and other Ci transporters) should otherwise allow *LCIB* mutants to survive in low CO_2 as it does in very low CO_2. This CO_2 inhibition appears to occur very quickly, because it can be seen almost immediately after Ci concentrations exceed the inhibitory CO_2 concentration

in photosynthetic O_2 evolution measurements. If CO_2 is responsible for the apparent inhibition of LCIA activity, this inhibition could be caused directly by CO_2 itself or through an unidentified CO_2 sensor protein, and this inhibition might extend to other target proteins, such as other Ci transporters. If this inhibition occurs and impacts survivability of *LCIB* mutants in air CO_2 level (i.e. is responsible for the *air dier* phenotype), it must take place at the post-translational or allosteric level, because it occurs so rapidly, and because no significant changes beyond those detected in low CO_2 conditions have been detected for *LCIA* or other potential Ci transporter genes at the transcriptional level under very low CO_2 conditions, (Brueggeman et al., 2012; Fang et al., 2012).

We can use logic similar to that we used to calculate the contribution of LCIA to *ad1*, and plot the apparent contribution of LCIB to photosynthetic O_2 evolution of the wild-type strain *cw10* (i.e. subtract the O_2 evolution rate of *ad1* from that of *cw10*). If we then compare that calculated LCIB contribution with the apparent contribution of LCIA to *ad1* (Fig. 7C), it becomes evident that the apparent LCIA contribution declines at CO_2 concentrations where the apparent LCIB contribution becomes substantial. This relationship would explain why LCIA and LCIB both contribute to growth in very low CO_2 but only LCIB appears essential for growth in low CO_2 (e.g. air level of CO_2).

Distinct Roles Played by LCIA and LCIB in Low CO_2 and Very Low CO_2 Acclimation States

Because of slow diffusion of CO_2 in water, Ci concentration can often change dramatically on a daily basis in an aquatic environment, especially in the natural soil environment of *C. reinhardtii* when cell population increases and photosynthesis activities are high. The presence of multiple limiting CO_2 acclimation states in microalgae may reflect an evolutionary adaptation to this aspect of their natural habitats. The apparent inhibition of LCIA activity by CO_2 concentrations at and above air level, together with the subcellular localizations of and apparent complementary roles for LCIA and LCIB (Fig. 8), suggest a possible explanation for how and why *C. reinhardtii* acclimates to different limiting CO_2 conditions. Figure 8 illustrates a proposed working model that could explain the functions of LCIA and LCIB in the *C. reinhardtii* CCM in these two acclimation states.

In this hypothetical model, at very low CO_2 (Fig. 8A), both LCIB and LCIA contribute to Ci accumulation. An LCIA-associated HCO_3^- transport pathway is largely responsible for HCO_3^- uptake into the chloroplast, possibly in concert with other HCO_3^- transporter(s) on the plasma membrane and/or the chloroplast envelope. LCIB, located around the pyrenoid, traps CO_2, either escaping from the pyrenoid or entering from outside the cell, into the stromal HCO_3^- pool. This stromal HCO_3^- pool then provides substrate to the pyrenoid thylakoid tubules for CAH3-catalyzed dehydration to CO_2 for Rubisco, as described in previous CCM models (Spalding et al., 1983b; Mitra et al., 2005; Spalding, 2008; Moroney et al., 2011).

In low CO_2 (Fig. 8B), the majority of LCIB protein complex in chloroplasts are located throughout the stromal space. In this condition, the hypothetical model predicts that LCIB-associated CO_2 uptake into the stromal HCO_3^- pool plays a more dominant role, and Ci uptake associated with LCIA and other HCO_3^- transporters is inhibited by CO_2 in the low CO_2 concentration range. Again, the stromal HCO_3^- accumulated through LCIB activity provides substrate to the pyrenoid thylakoid tubules for CAH3-catalyzed dehydration to CO_2 for Rubisco as described in previous CCM models.

Assuming that the LCIB-mediated CO_2 uptake system provides an adequate supply of substrate CO_2 for Rubisco in the low CO_2 range and that simple CO_2 diffusion can do so at higher CO_2 concentrations, such CO_2 inhibition of HCO_3^- transport at air concentrations

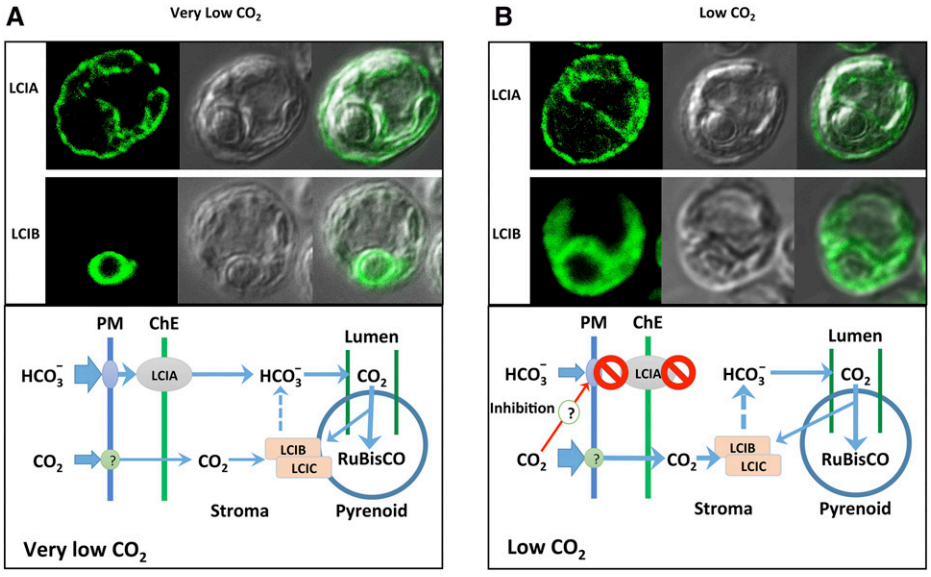

Figure 8. Models for acclimation to low and very low CO_2 in *C. reinhardtii*. A and B, Immunolocalization of LCIA and LCIB and working models illustrating possible roles played by the LCIA-associated HCO_3^- uptake system and the LCIB-associated CO_2 uptake system in very low CO_2 grown cells (A) and low CO_2 grown cells (B). No obvious changes of LCIA localization were observed between low and very low CO_2 conditions. Dashed lines represent the hypothesized function of the LCIB-LCIC complex in conversion of CO_2 to HCO_3^-, which is then delivered to CAH3 within the lumen of the pyrenoid-associated thylakoid tubules for dehydration to CO_2. A detailed explanation is provided in "Discussion." ChE, Chloroplast envelope; PM, plasma membrane.

and above may reflect a versatile regulatory mechanism present in eukaryotic algae for acclimating quickly to changes in CO_2 availability that frequently occur in their natural environments. By switching rapidly from energy-intensive HCO_3^- transport systems to a CO_2 uptake system (possibly energetically less costly) when CO_2 becomes more abundant, algae cells can divert more solar energy for photosynthetic carbon fixation and other metabolic reactions to enable faster growth at a lower energy cost.

The well-documented regulation by transcript abundance should prevent even the synthesis of the HCO_3^- transporters under high CO_2 conditions, in which the transporters clearly are not needed. However, in lower CO_2 concentration ranges, such as 5 to 50 μM (0.015%–0.15%) CO_2, it may be advantageous for the cells to have the capacity to respond quickly to either activate or inactivate HCO_3^- transport in response to CO_2 availability. Fluctuations in CO_2 concentration near the surface of the natural soil environment of *C. reinhardtii* may occur over time frames too short for transcriptional regulation to act effectively, but the post-translational or allosteric regulation proposed here would allow HCO_3^- transporters to shift rapidly between active and inactive states in response to CO_2 concentration fluctuations. Further research will be required to determine whether this rapid regulation actually occurs via CO_2 inhibition of the CCM HCO_3^- transporter pathway.

MATERIALS AND METHODS

Cultures and Growth Conditions

The wild-type strain *cw10* (CC849) and CC620 and the mutant strains of *Chlamydomonas reinhardtii* were maintained and grown as previously described (Wang and Spalding, 2006). For inducing very low CO_2 acclimation, liquid cell cultures were first grown in minimal medium (pH 7.3) to late log phase in high CO_2 gas (5% CO_2 [v/v] in air), and then switched to very low CO_2 by bubbling very low CO_2 gas though the liquid phase for 20 to 24 h. The very low CO_2 (0.008%–0.01%) gas was obtained by passing normal air through a saturated sodium hydroxide solution and remixing with normal air to achieve the desired final concentration.

Isolation of Mutants, Identification of Mutation, and Genetic Analysis

Spot growth testing, mutant screening, and transformation were performed as previously described (Wang and Spalding, 2006). Strain *ad1* was transformed with linearized pSI103d plasmid (Sizova et al., 2001). Transformed cells were kept in high CO_2 and selected on minimal medium plates supplemented with 10 μg mL^{-1} paromomycin. Paromomycin-resistant transformants were transferred to duplicate plates for screening by growth spot tests in high CO_2 and very low CO_2.

The genomic DNA fragments flanking the insertion in mutants were identified by the restriction enzyme site-directed amplification PCR (González-Ballester et al., 2005). The primary PCR was carried out in a volume of 25 μL containing 2.5 μL of 10× PCR buffer (Invitrogen), 0.25 μL of Taq polymerase (Invitrogen), 1 μL of 25 mM $MgCl_2$, 0.4 μL of 10 mM deoxynucleotides, 0.75 μL of dimethyl sulfoxide, 5 pmol of primer RB1, 15 pmol of degenerate primers (González-Ballester et al., 2005), and 50 ng of genomic DNA as the DNA template. The secondary PCR was carried out in a volume of 25 μL with the same reagents as the primary RCR except 5 pmol of Q_0 primer was used to replace the degenerate primers and 1 μL of 25:1 diluted PCR product from the primary reaction was used as the DNA template. The parameters for the PCR cycle were set up according to Dent et al. (2005).

The genetic crosses between *lab1* and CC620 were performed according to Harris (2009). The progeny bearing both *Ble* and *Aph8* were selected on agar plates made from Tris-acetate-phosphate medium supplemented with 10 μg mL^{-1} paromomycin and 10 μg mL^{-1} zeocin. The progeny bearing only *Aph8* was selected on agar medium supplemented with 10 μg mL^{-1} paromomycin, and then their zeo^R was tested on plates supplemented with 10 μg mL^{-1} of zeocin. PCR amplification with primers specific for *LCIB* or *LCIA* was used to confirm the defects in *LCIA* or *LCIB* in these progeny. To complement *lab1*, a genomic DNA fragment including the *LCIA* coding sequence, putative promoter region, and 3′ UTR was cloned into pBluescript vector, and used to transform *lab1*. The successful transformants were directly selected in very low CO_2 on minimal medium plates and untransformed *lab1* was used as the control. The genomic DNA from the transformants was isolated and PCR amplified with specific primers in the region of *LCIA* where the insertion is located.

Measurements of Photosynthetic O_2 Evolution

Photosynthetic O_2 evolution was measured at 25°C with a Clark-type oxygen electrode controlled by an Oxy-Lab unit (Hansatech). Cells from liquid cultures were collected by centrifugation and suspended in 4 mL of N_2-saturated buffers to a final chlorophyll concentration of 20 μg mL^{-1}. The buffers used were MOPS-Tris (25 mM, pH 7.3), MES-KOH (25 mM, pH 6.0), or AMPSO (25 mM, pH 9.0). For each cell preparation, internal and external Ci were depleted under illumination (500 μmol photons m^{-2} s^{-1}) as judged by cessation of O_2 evolution before each measurement. The Ci-dependent O_2 evolution was initiated by addition of various concentrations of $NaHCO_3$. For most measurements, the subsequent addition of Ci was delayed until the previous O_2 evolution rate approached zero. When O_2 evolution rates were extremely slow, such as in high pH or in *lab1* mutants, the subsequent Ci was added to a desired concentration after previous O_2 evolution proceeded at least 1 min or longer; and the Ci concentration at each next addition was calculated based on the amount of Ci consumed from the previous Ci addition as reflected by the amount of O_2 evolved. Because O_2, when reaching high levels, appears to have negative influence on photosynthesis, the O_2 level in cell suspension was kept low by flushing with N_2 gas when it exceeded 200 nmol mL^{-1}. Two hundred units per milliliter of bovine CA (C2624; Sigma) was present in the measurements at pH 6.0 and 7.3 to ensure the equilibrium of CO_2 and HCO_3^-.

Western-Blot Analysis and Immunolocalization

For protein analyses, harvested cells were directly dissolved in a 1× SDS-PAGE buffer in the presence of 2-mercaptoethanol at 80°C for 5 min. The resulting lysates were passed through a 26-gauge needle to reduce viscosity and then separated on 12% (v/v) SDS-polyacrylamide gels. Immunoblotting with specific antibodies was performed to detect the specific proteins by chemiluminescence (SuperSignal Wester Pico; Thermo Scientific).

To generate LCIA-specific antibodies, five *LCIA* complementary DNA fragments encoding different predicted soluble portions in LCIA protein were PCR amplified from a complementary DNA library (Wang and Spalding, 2006) and combined by recombination PCR. The resulting mini-LCIA sequence was cloned into pET-28a vector, and transformed into BL21 (DE3) *Escherichia coli* cells for overexpression. The expressed mini-LCIA was purified from *E. coli* and used to raise LCIA polyclonal antiserum. An LCIA monoclonal antibody against a synthetic peptide ENAINVGAYK was also generated (Abmart). LCIB antiserum against purified LCIB was previously described (Duanmu et al., 2009b). LCI1 antiserum was a gift from James V. Moroney (Louisiana State University).

For immunolocalization, cell suspension was placed on precharged microscope slides (ProbeOn Plus; FisherBiotech) for 1 to 3 min, and then quickly fixed in −20°C methanol for 10 min. Immunofluorescence staining was performed according to Cole et al. (1998). Antiserum against LCIA or LCIB was used at a dilution of 1:1,000 as primary antibody, and fluorescein isothiocyanate-conjugated goat anti-rabbit IgG or goat anti-mouse IgG (Jackson ImmunoResearch Laboratories) was used at a dilution of 1:150 as the secondary antibody for immunofluorescence. After final washing with phosphate-buffered saline, the slides were mounted using ProLong Gold reagents (Invitrogen), and digital images of stained cells were acquired with a Leica SP5 X MP confocal microscope.

ACKNOWLEDGMENTS

We thank Dr. James V. Moroney (Department of Biological Sciences, Louisiana State University) for the kind gift of LCI1 antibody and Dr. Deqiang Duanmu (Department of Molecular Biosciences, University of California, Davis) for advice on the article.

Received August 10, 2014; accepted October 17, 2014; published October 21, 2014.

LITERATURE CITED

Amoroso G, Sultemeyer D, Thyssen C, Fock HP (1998) Uptake of HCO_3^- and CO_2 in cells and chloroplasts from the microalgae *Chlamydomonas reinhardtii* and *Dunaliella tertiolecta*. Plant Physiol **116:** 193–201

Badger M, Spalding M (2000) CO_2 Acquisition, Concentration and Fixation in Cyanobacteria and Algae. Kluwer Academic, Dordrecht, The Netherlands

Badger MR, Price GD (2003) CO_2 concentrating mechanisms in cyanobacteria: molecular components, their diversity and evolution. J Exp Bot **54:** 609–622

Behrenfeld MJ, Randerson JT, McClain CR, Feldman GC, Los SO, Tucker CJ, Falkowski PG, Field CB, Frouin R, Esaias WE, et al (2001) Biospheric primary production during an ENSO transition. Science **291:** 2594–2597

Brueggeman AJ, Gangadharaiah DS, Cserhati MF, Casero D, Weeks DP, Ladunga I (2012) Activation of the carbon concentrating mechanism by CO_2 deprivation coincides with massive transcriptional restructuring in *Chlamydomonas reinhardtii*. Plant Cell **24:** 1860–1875

Cole DG, Diener DR, Himelblau AL, Beech PL, Fuster JC, Rosenbaum JL (1998) *Chlamydomonas* kinesin-II-dependent intraflagellar transport (IFT): IFT particles contain proteins required for ciliary assembly in *Caenorhabditis elegans* sensory neurons. J Cell Biol **141:** 993–1008

Demmig B, Gimmler H (1983) Properties of the isolated intact chloroplast at cytoplasmic K^+ concentrations: I. Light-induced cation uptake into intact chloroplasts is driven by an electrical potential difference. Plant Physiol **73:** 169–174

Dent RM, Haglund CM, Chin BL, Kobayashi MC, Niyogi KK (2005) Functional genomics of eukaryotic photosynthesis using insertional mutagenesis of *Chlamydomonas reinhardtii*. Plant Physiol **137:** 545–556

Duanmu D, Miller AR, Horken KM, Weeks DP, Spalding MH (2009a) Knockdown of limiting-CO_2-induced gene *HLA3* decreases HCO_3^- transport and photosynthetic Ci affinity in *Chlamydomonas reinhardtii*. Proc Natl Acad Sci USA **106:** 5990–5995

Duanmu D, Spalding MH (2011) Insertional suppressors of *Chlamydomonas reinhardtii* that restore growth of *air-dier lcib* mutants in low CO_2. Photosynth Res **109:** 123–132

Duanmu D, Wang Y, Spalding MH (2009b) Thylakoid lumen carbonic anhydrase (*CAH3*) mutation suppresses air-dier phenotype of *LCIB* mutant in *Chlamydomonas reinhardtii*. Plant Physiol **149:** 929–937

Fang W, Si Y, Douglass S, Casero D, Merchant SS, Pellegrini M, Ladunga I, Liu P, Spalding MH (2012) Transcriptome-wide changes in *Chlamydomonas reinhardtii* gene expression regulated by carbon dioxide and the CO_2-concentrating mechanism regulator *CIA5/CCM1*. Plant Cell **24:** 1876–1893

Fuks B, Homblé F (1999) Passive anion transport through the chloroplast inner envelope membrane measured by osmotic swelling of intact chloroplasts. Biochim Biophys Acta **1416:** 361–369

González-Ballester D, de Montaigu A, Galván A, Fernández E (2005) Restriction enzyme site-directed amplification PCR: a tool to identify regions flanking a marker DNA. Anal Biochem **340:** 330–335

Harris EH (2009) The *Chlamydomonas* Sourcebook. Academic Press, Oxford

Im CS, Grossman AR (2002) Identification and regulation of high light-induced genes in *Chlamydomonas reinhardtii*. Plant J **30:** 301–313

Lü W, Du J, Schwarzer NJ, Gerbig-Smentek E, Einsle O, Andrade SL (2012b) The formate channel FocA exports the products of mixed-acid fermentation. Proc Natl Acad Sci USA **109:** 13254–13259

Lü W, Du J, Schwarzer NJ, Wacker T, Andrade SLA, Einsle O (2013) The formate/nitrite transporter family of anion channels. Biol Chem **394:** 715–727

Lü W, Schwarzer NJ, Du J, Gerbig-Smentek E, Andrade SL, Einsle O (2012a) Structural and functional characterization of the nitrite channel NirC from Salmonella typhimurium. Proc Natl Acad Sci USA **109:** 18395–18400

Mariscal V, Moulin P, Orsel M, Miller AJ, Fernández E, Galván A (2006) Differential regulation of the *Chlamydomonas Nar1* gene family by carbon and nitrogen. Protist **157:** 421–433

Mitra M, Mason CB, Xiao Y, Ynalvez RA, Lato SM, Moroney JV (2005) The carbonic anhydrase gene families of *Chlamydomonas reinhardtii*. Can J Bot **83:** 780–795

Miura K, Yamano T, Yoshioka S, Kohinata T, Inoue Y, Taniguchi F, Asamizu E, Nakamura Y, Tabata S, Yamato KT, et al (2004) Expression profiling-based identification of CO_2-responsive genes regulated by CCM1 controlling a carbon-concentrating mechanism in *Chlamydomonas reinhardtii*. Plant Physiol **135:** 1595–1607

Moroney JV, Ma Y, Frey WD, Fusilier KA, Pham TT, Simms TA, DiMario RJ, Yang J, Mukherjee B (2011) The carbonic anhydrase isoforms of *Chlamydomonas reinhardtii*: intracellular location, expression, and physiological roles. Photosynth Res **109:** 133–149

Moroney JV, Mason CB (1991) The Role of the chloroplast in inorganic carbon acquisition by *Chlamydomonas reinhardtii*. Can J Bot **69:** 1017–1024

Moroney JV, Tolbert NE (1985) Inorganic carbon uptake by *Chlamydomonas reinhardtii*. Plant Physiol **77:** 253–258

Moroney JV, Ynalvez RA (2007) Proposed carbon dioxide concentrating mechanism in *Chlamydomonas reinhardtii*. Eukaryot Cell **6:** 1251–1259

Ohnishi N, Mukherjee B, Tsujikawa T, Yanase M, Nakano H, Moroney JV, Fukuzawa H (2010) Expression of a low CO_2-inducible protein, LCI1, increases inorganic carbon uptake in the green alga *Chlamydomonas reinhardtii*. Plant Cell **22:** 3105–3117

Pollock SV, Prout DL, Godfrey AC, Lemaire SD, Moroney JV (2004) The *Chlamydomonas reinhardtii* proteins Ccp1 and Ccp2 are required for long-term growth, but are not necessary for efficient photosynthesis, in a low-CO_2 environment. Plant Mol Biol **56:** 125–132

Price GD, Badger MR, Woodger FJ, Long BM (2008) Advances in understanding the cyanobacterial CO_2-concentrating-mechanism (CCM): functional components, Ci transporters, diversity, genetic regulation and prospects for engineering into plants. J Exp Bot **59:** 1441–1461

Price GD, Maeda S, Omata T, Badger MR (2002) Modes of active inorganic carbon uptake in the cyanobacterium, *Synechococcus* sp. PCC7942. Funct Plant Biol **29:** 131–149

Ramazanov Z, Mason CB, Geraghty AM, Spalding MH, Moroney JV (1993) The low CO_2-inducible 36-kilodalton protein is localized to the chloroplast envelope of *Chlamydomonas reinhardtii*. Plant Physiol **101:** 1195–1199

Sheehan J, Dunahay T, Benemann J, Roessler P (1998) A Look Back at the U.S. Department of Energy's Aquatic Species Program: Biodiesel from Algae. Report No. NREL/TP-580-24190. National Renewable Energy Laboratory, Golden, CO

Sizova I, Fuhrmann M, Hegemann P (2001) A *Streptomyces rimosus aphVIII* gene coding for a new type phosphotransferase provides stable antibiotic resistance to *Chlamydomonas reinhardtii*. Gene **277:** 221–229

Spalding MH (2008) Microalgal carbon-dioxide-concentrating mechanisms: *Chlamydomonas* inorganic carbon transporters. J Exp Bot **59:** 1463–1473

Spalding MH, Ogren WL (1983) Evidence for a saturable transport component in the inorganic carbon uptake of *Chlamydomonas reinhardii*. FEBS Lett **154:** 335–338

Spalding MH, Spreitzer RJ, Ogren WL (1983a) Reduced inorganic carbon transport in a CO_2-requiring mutant of *Chlamydomonas reinhardii*. Plant Physiol **73:** 273–276

Spalding MH, Spreitzer RJ, Ogren WL (1983b) Carbonic anhydrase-deficient mutant of *Chlamydomonas reinhardii* requires elevated carbon dioxide concentration for photoautotrophic growth. Plant Physiol **73:** 268–272

Spalding MH, Van K, Wang Y, Nakamura Y (2002) Acclimation of *Chlamydomonas* to changing carbon availability. Funct Plant Biol **29:** 221–230

Sültemeyer DF, Klöck G, Kreuzberg K, Fock HP (1988) Photosynthesis and apparent affinity for dissolved inorganic carbon by cells and chloroplasts of *Chlamydomonas reinhardtii* grown at high and low CO_2 concentrations. Planta **176:** 256–260

Sültemeyer DF, Miller AG, Espie GS, Fock HP, Canvin DT (1989) Active CO_2 transport by the green-alga *Chlamydomonas reinhardtii*. Plant Physiol **89:** 1213–1219

Vance P, Spalding MH (2005) Growth, photosynthesis and gene expression in *Chlamydomonas* over a range of CO_2 concentrations and CO_2/O_2 ratios: CO_2 regulates multiple acclimation states. Can J Bot **85:** 796–805

Wang Y, Duanmu D, Spalding MH (2011) Carbon dioxide concentrating mechanism in *Chlamydomonas reinhardtii*: inorganic carbon transport and CO_2 recapture. Photosynth Res **109:** 115–122

Wang Y, Huang Y, Wang J, Cheng C, Huang W, Lu P, Xu YN, Wang P, Yan N, Shi Y (2009) Structure of the formate transporter FocA reveals a pentameric aquaporin-like channel. Nature **462:** 467–472

Wang Y, Spalding MH (2006) An inorganic carbon transport system responsible for acclimation specific to air levels of CO_2 in *Chlamydomonas reinhardtii*. Proc Natl Acad Sci USA **103:** 10110–10115

Wang Y, Spalding MH (2014) LCIB in the *Chlamydomonas* CO_2-concentrating mechanism. Photosynth Res **121:** 185–192

Wijffels RH, Barbosa MJ (2010) An outlook on microalgal biofuels. Science **329:** 796–799

Wu W, Peters J, Berkowitz GA (1991) Surface charge-mediated effects of Mg^{2+} on K^+ flux across the chloroplast envelope are associated with regulation of stromal pH and photosynthesis. Plant Physiol **97:** 580–587

Yamano T, Asada A, Sato E, Fukuzawa H (2014) Isolation and characterization of mutants defective in the localization of LCIB, an essential factor for the carbon-concentrating mechanism in *Chlamydomonas reinhardtii*. Photosynth Res **121:** 193–200

Yamano T, Tsujikawa T, Hatano K, Ozawa S, Takahashi Y, Fukuzawa H (2010) Light and low-CO_2-dependent LCIB-LCIC complex localization in the chloroplast supports the carbon-concentrating mechanism in *Chlamydomonas reinhardtii*. Plant Cell Physiol **51:** 1453–1468